

Realization of high tunability barium strontium titanate thin films by rf magnetron sputtering

P. Padmini,^{a)} T. R. Taylor,^{b)} M. J. Lefevre,^{b)} A. S. Nagra,^{a)} R. A. York,^{a)}
and J. S. Speck^{b),c)}

College of Engineering, University of California, Santa Barbara, California 93106

(Received 21 July 1999; accepted for publication 23 September 1999)

Ferroelectric thin films are currently being used to develop tunable microwave circuits based on the electric-field dependence of the dielectric constant. $(\text{Ba}_{0.5}\text{Sr}_{0.5})\text{TiO}_3$ (BST) films prepared by sputtering on Pt/TiO₂/SiO₂/Si substrates are found to exhibit a capacitance change (tunability) of nearly 4:1. Higher tunability has been attributed to the (100) texturing of the BST films and is a result of the biaxial tensile stress imposed by Si on BST making the polar axis oriented in plane. Electrical characterization shows that the dielectric permittivity increases with increase in film thickness (up to ~ 200 nm). © 1999 American Institute of Physics. [S0003-6951(99)03646-3]

Ferroelectric thin films based on $(\text{Ba}_{0.5}\text{Sr}_{0.5})\text{TiO}_3$ (BST) are potential candidates for applications as the storage capacitor dielectric for future generation dynamic random access memory (DRAM)¹ because of its high dielectric constant. As a result of the development of BST for the DRAM industry, it was found that the dielectric permittivity has a strong field dependence, where typically the permittivity decreases with increasing field. However, the DRAM efforts have not been concerned with tunability or other properties important for microwave circuits. The field-dependent change of the dielectric permittivity can be used for microwave and millimeter-wave applications such as tunable filters, matching networks, and phase delay elements in traveling-wave or transmission-line structures.^{2,3} In most cases, low loss tangents and high dielectric tunability will be required, where tunability is defined as $\epsilon_{r(\text{max})}/\epsilon_{r(\text{min})}$. The relative dielectric constant at zero bias is represented by $\epsilon_{r(\text{max})}$, and $\epsilon_{r(\text{min})}$ is the relative dielectric constant at a higher or defined field.

Our main focus has been to optimize sputtered BST films for higher tunability to be used in applications such as varactors-diode replacements in transmission lines and as the nonlinear medium in frequency triplers. Capacitors with high tunability can reduce the physical dimensions and circuit losses of a transmission line structure, and increase the conversion efficiency of frequency triplers. The field dependence of dielectric constant has been modeled as an interfacial layer in series with a bulk layer.⁴ Both the interfacial and bulk layers have nonlinear dielectric response, with the interfacial layer having a lower dielectric permittivity than the bulk of the film. This letter discusses the dependence of tunability on the texture of the film. We report a capacitance change of nearly 4:1 for sputtered polycrystalline films. However, higher tunabilities of nearly 6:1 have been observed for films deposited by chemical vapor deposition (CVD).⁴

In sputtered BST films, the (100) texture has been found

to give a high tunability, while its growth kinetics is poorly understood. It is well known that the dielectric properties of BST films depend on the dielectric-electrode interface, the stress state of the film, microstructure, texture as well as surface morphology. An understanding of the nucleation and growth kinetics is required to control the microstructure to achieve device quality thin films. Stress in the film can result from the difference in the thermal expansion coefficients between the substrate, electrode and the film. This biaxial strain can give rise to a quasi polarization^{5,6} that has been attributed as one of the possible causes of ferroelectric suppression in BST thin films. Other possible reasons for the disappearance of ferroelectricity in BST thin films include: grain size effects, interfacial chemical reactions, and interdiffusion between the substrate and the film.⁷⁻⁹

BST films were sputtered from a stoichiometric $(\text{Ba}_{0.5}\text{Sr}_{0.5})\text{TiO}_3$ target onto Pt (100 nm)/TiO₂ (100 nm)/SiO₂ (100 nm)/Si substrates under the conditions listed in Table I. Pt [(111) textured] and TiO₂ were sputter deposited at 400 °C (Silicon Quest, Santa Clara, California). The substrates were ultrasonically cleaned with acetone and isopropanol prior to BST deposition. The films were structurally characterized by x-ray diffraction, scanning and transmission electron microscopy. Ni-filtered Cu $K\alpha$ radiation with a detector slit size of $\frac{1}{2}^\circ$, slit height of about 2 mm, and step size of 0.02° , was used to determine the texture of the BST films by x-ray diffraction (Philips XPert x-ray diffractometer). The composition of the films was verified by Rutherford backscattering spectroscopy (RBS). Films prepared at an Ar/O₂ of 180/10 had a composition within an error of 1% (Ba/Sr = 0.49/0.51) of the target (Ba/Sr = 0.5/0.5). The surface

TABLE I. Sputtering conditions for BST deposition.

Target	$\text{Ba}_{0.5}\text{Sr}_{0.5}\text{TiO}_3$
Target diameter	3 in.
Source to substrate distance	4 in.
RF power	90 W
Sputtering gas	Ar/O ₂ (sccm)
Substrate temperature	450–650 °C
Gas pressure	50 mT
Deposition rate	0.4 nm/min

^{a)}Department of Electrical and Computer Engineering.

^{b)}Department of Materials.

^{c)}Electronic mail: speck@mrl.ucsb.edu

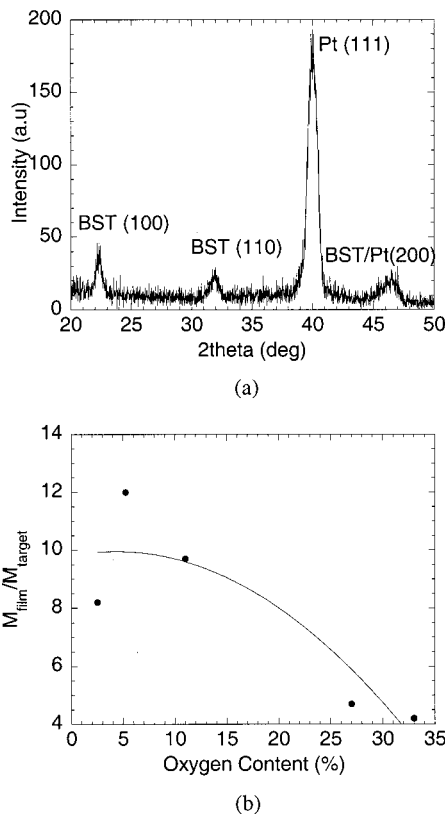


FIG. 1. (a) X-ray diffraction of 72 nm BST film sputtered at an Ar/O₂ of 180/10, sputtering pressure of 50 mT and deposition temperature of 550 °C. (b) Ratio of texturing as a function of the oxygen content in the Ar/O₂ gas mixture.

roughness of the BST films analyzed by atomic force microscopy (AFM) were found to be ~1.5–1.7 nm, which is typical of polycrystalline films.¹⁰ The film thickness was measured by RBS, cross-sectional transmission electron microscopy (TEM) as well as variable angle spectroscopic ellipsometry (VASE). Pt top electrodes were evaporated onto the BST through a shadow mask to define capacitors for electrical testing. Capacitance–voltage measurements were done at 1 MHz using an HP4145 impedance analyzer. All measurements were done as cycle sweeps (negative voltage to positive voltage back to negative voltage) to check for any possible hysteretic behavior.

The x-ray diffraction pattern of a BST film [Fig. 1(a)] sputtered at 550 °C substrate temperature and at an Ar/O₂ of 90/10, exhibit a phase pure crystalline film, which is predominantly (100) oriented. Cross-sectional TEM images of the corresponding film shows a columnar structure with a lateral grain size of 10–15 nm, similar to that reported for films grown by CVD.^{4,11} Figure 1(b) shows the effect of the oxygen content in the plasma on the texturing ratio, for 72 nm thick films deposited at 50 mTorr and 475 °C substrate temperature. The texturing ratio is defined as $M_{\text{film}}/M_{\text{target}}$, where

$$M_{\text{film}} = I_{(100)} / [I_{(100)} + I_{(110)}],$$

$$M_{\text{target}} = I_{(100)} / [I_{(100)} + I_{(110)}].$$

$I_{(hkl)}$ is the integrated intensity of the (hkl) peaks recorded in θ – 2θ scans. The overlap of (111) BST peak and the (111)Pt peak precluded the use of (111) reflections in our

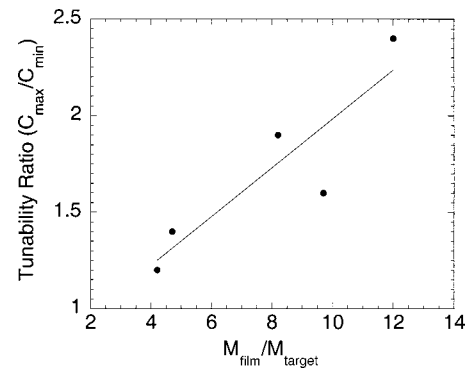


FIG. 2. Tunability as a function of texturing ratio.

texture factors. It can be observed that the (100) texturing has a maximum at an Ar/O₂ ratio of 180/10. The nucleation and growth kinetics for the preferred orientation is not well understood and further studies are in progress.

Figure 2 shows the variation in tunability as a function of texturing ratio over a –5 to +5 V bias sweep. The films were 72 nm thick and a maximum tunability is obtained at an Ar/O₂ of 180/10. Higher tunability has been attributed to the (100) texture of the film. Figure 3(a) shows the variation of dielectric permittivity, calculated from the room temperature capacitance–voltage data as a function of film thickness. The increase in dielectric constant with thickness has been previously attributed to the increase in grain size for thicker films.¹² However, a plot of zero bias dielectric constant versus thickness [Fig. 3(b)] reveals that the permittivity saturates for film thickness greater than >200 nm. If the dielectric constant is a function of composition and is independent

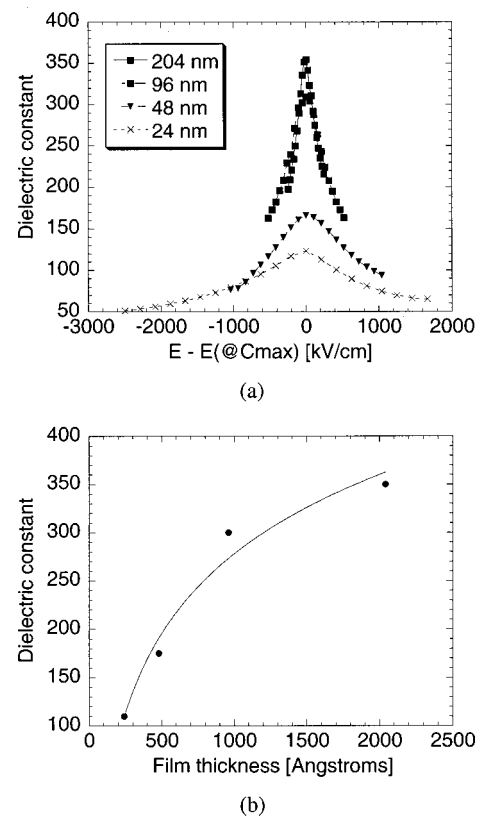


FIG. 3. (a) Apparent dielectric permittivity vs electric field for BST films of varying thickness. (b) Dielectric permittivity as a function of film thickness.

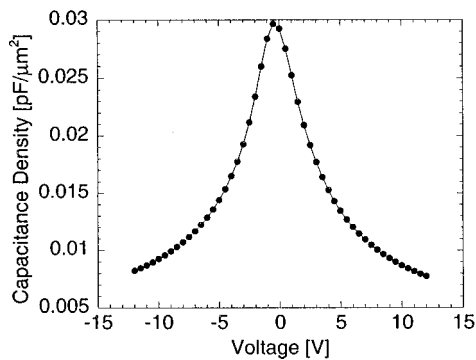


FIG. 4. Capacitance–voltage characteristics of a 72 nm BST film showing a capacitance change of nearly 4:1.

of the film thickness, then the observed saturation in dielectric constant above a certain thickness can only be explained by the presence of an interfacial capacitance layer. Therefore, thicker films are influenced less by the interfacial layer since the behavior is described by two capacitors in series. The interfacial layer can be thought of to arise from the reaction layers at the film/electrode interface, changes in the defect chemistry at the dielectric–electrode interface, or it may be associated with intrinsic issues in local compatibility across the dielectric–electrode interface.^{13–15} Further studies have to be carried out to clarify the origin of the thickness dependence.

Figure 4 shows the capacitance–voltage behavior of a 72 nm BST film prepared at a 550 °C substrate temperature, 50 mTorr, and an Ar/O₂ of 180/10. A capacitance change of about 4:1 is observed. Improved tunability has been attributed to the (100) texture of the film leading to an enhancement of the in-plane oriented polar axis. When polar materials are subjected to tensile stress, a contraction occurs along the *c* axis leading to an enhancement in its in-plane orientation; making the *a* axis parallel to the film normal. In a proper tetragonal ferroelectric, the permittivity along the polar axis (*c* axis) is much less in comparison to that along the nonpolar axis (*a* axis). Hence, the lowering of the dielectric permittivity at higher voltages or fields can be interpreted as a result of quasi poling with the *c*-axis switched out of plane. It has been shown by Pertsev *et al.*^{5,6} that when the substrate imposes a biaxial tension on the paraelectric phase, the in-plane orientation of the polar axis appears to be energetically

favorable with respect to the elastic contribution to the film free energy.

In summary, this letter has demonstrated how sputtered (100) textured BST thin films show increased tunability. Film growth on substrates that give rise to biaxial tension in the film (e.g., $\alpha_{\text{sub}} < \alpha_{\text{film}}$, where α is the thermal coefficient of expansion) results in the polar axis of the material orienting itself along the substrate surface. The in-plane orientation of the polar axis yields BST films with higher tunability. Further studies are necessary to explore the nucleation and growth kinetics of sputtered BST films, the origin of the film's thickness dependence, and the impact of stress and interface reactions on the microwave properties of BST sputtered films. In addition, an explanation has to be found for the maximum permittivity offset from zero bias, presumably due to built in electric field.

This research has been supported by DARPA through the Frequency Agile Materials for Electronics Program (FAME) under Award No. DABT63-98-1-0006. The authors would like to thank Dr. Stephen Streiffer, Dr. Orlando Auciello, and Dr. Jaemo Im of Argonne National Labs for the RBS data and valuable input.

¹D. E. Kotecki, *Integr. Ferroelectr.* **16**, 1 (1997).

²De Flaviis, N. G. Alexopoulos, and M. Staffsudd, *IEEE Trans. Microwave Theory Tech.* **45**, 963 (1997).

³V. K. Varadan, D. K. Ghodgaonker, V. V. Varadan, J. F. Kelly, and P. Glikerdas, *Microwave J.* **35**, 116 (1992).

⁴C. Basceri, S. K. Streiffer, A. I. Kingon, and R. Waser, *J. Appl. Phys.* **82**, 2497 (1997).

⁵N. A. Pertsev, A. G. Zembilgotov, S. Hoffmann, R. Waser, and A. K. Tagantsev, *J. Appl. Phys.* **85**, 1698 (1999).

⁶N. A. Pertsev, A. G. Zembilgotov, and A. K. Tagantsev, *Phys. Rev. Lett.* **80**, 1988 (1998).

⁷V. S. Dharmadhikari and W. W. Grannemann, *J. Vac. Sci. Technol. A* **1**, 483 (1983).

⁸Y. G. Wang, W. L. Zhong, and P. L. Zhang, *Phys. Rev. B* **51**, 5311 (1995).

⁹J. W. Jang, S. J. Chung, W. J. Cho, T. S. Hahn, and S. S. Choi, *J. Appl. Phys.* **81**, 6322 (1997).

¹⁰M. S. Tsai, S. C. Sun, and T. Y. Tseng, *J. Appl. Phys.* **82**, 3482 (1997).

¹¹S. Stemmer, S. K. Streiffer, N. D. Browning, and A. I. Kingon, *Appl. Phys. Lett.* **74**, 2432 (1999).

¹²R. Waser, *Integr. Ferroelectr.* **15**, 39 (1997).

¹³I. P. Batra, P. Wurfel, and B. D. Silverman, *Phys. Rev. B* **55**, 1206 (1997).

¹⁴C. Zhou and D. M. Newns, *J. Appl. Phys.* **82**, 3081 (1997).

¹⁵G. W. Dietz, M. Schumacher, R. Waser, S. K. Streiffer, C. Basceri, and A. I. Kingon, *J. Appl. Phys.* **82**, 2359 (1997).